

Gray and White Matter Abnormalities in Treated Human Immunodeficiency Virus Disease and Their Relationship to Cognitive Function

Jonathan Underwood,¹ James H. Cole,² Matthan Caan,³ Davide De Francesco,⁴ Robert Leech,² Rosan A. van Zoest,⁵ Tanja Su,³ Gert J. Geurtsen,⁶ Ben A. Schmand,⁶ Peter Portegies,⁷ Maria Prins,⁸ Ferdinand W. N. M. Wit,^{5,9,10} Caroline A. Sabin,⁴ Charles Majoie,³ Peter Reiss,^{5,9,10} Alan Winston,^{1,a} and David J. Sharp^{2,a}; for the Comorbidity in Relation to AIDS (COBRA) Collaboration

Divisions of ¹Infectious Diseases and ²Brain Sciences, Imperial College London, United Kingdom; ³Department of Radiology, Academic Medical Center, Amsterdam, The Netherlands; ⁴Department of Infection and Population Health, University College London, United Kingdom; ⁵Department of Global Health, Academic Medical Center, and Amsterdam Institute for Global Health and Development; ⁶Department of Medical Psychology, and ⁷Department of Neurology, Academic Medical Center; ⁸Public Health Service Amsterdam, ⁹HIV Monitoring Foundation, and ¹⁰Department of Internal Medicine, Division of Infectious Diseases, Academic Medical Center, Amsterdam, The Netherlands

Background. Long-term comorbidities such as cognitive impairment remain prevalent in otherwise effectively treated people living with human immunodeficiency virus (HIV). We investigate the relationship between cognitive impairment and brain structure in successfully treated patients using multimodal neuroimaging from the Comorbidity in Relation to AIDS (COBRA) cohort.

Methods. Cognitive function, brain tissue volumes, and white matter microstructure were assessed in 134 HIV-infected patients and 79 controls. All patients had suppressed plasma HIV RNA at cohort entry. In addition to comprehensive voxelwise analyses of volumetric and diffusion tensor imaging, we used an unsupervised machine learning approach to combine cognitive, diffusion, and volumetric data, taking advantage of the complementary information they provide.

Results. Compared to the highly comparable control group, cognitive function was impaired in 4 of the 6 cognitive domains tested (median global T-scores: 50.8 vs 54.2; $P < .001$). Patients had lower gray but not white matter volumes, observed principally in regions where structure generally did not correlate with cognitive function. Widespread abnormalities in white matter microstructure were also seen, including reduced fractional anisotropy with increased mean and radial diffusivity. In contrast to the gray matter, these diffusion abnormalities correlated with cognitive function. Multivariate neuroimaging analysis identified a neuroimaging phenotype associated with poorer cognitive function, HIV infection, and systemic immune activation.

Conclusions. Cognitive impairment, lower gray matter volume, and white matter microstructural abnormalities were evident in HIV-infected individuals despite fully suppressive antiretroviral therapy. White matter abnormalities appear to be a particularly important determinant of cognitive dysfunction seen in well-treated HIV-infected individuals.

Keywords. HIV; cognitive impairment; neuroimaging; diffusion tensor imaging; voxel-based morphometry.

As a result of modern combination antiretroviral therapy (ART), human immunodeficiency virus (HIV) infection is now a chronic disease with life expectancy approaching that of the general population [1]. Despite this, concerns remain regarding an increased prevalence of age-associated comorbidities and the possibility of an “accelerated aging” phenotype [2]. Cognitive impairment, which is associated with poorer clinical outcomes and higher mortality [3, 4], reportedly affects up to 50% of

HIV-infected individuals [5, 6]. Yet, most data do not pertain to virologically suppressed cohorts, which are now the norm in Northern European settings [7], and hence there remains uncertainty about its aetiology.

One possibility is that cognitive impairment results from structural damage to brain regions that support cognition. Earlier work has described lower gray and white matter volumes in numerous locations in HIV-infected individuals [8–13]. Diffusion-weighted imaging, an advanced magnetic resonance imaging (MRI) technique, is more sensitive at revealing white matter abnormalities than volumetric measures in HIV-infected individuals [14–19]. However, the relationships between imaging abnormalities and cognitive function remain uncertain, particularly in well-treated patients, with several studies failing to report any associations [13, 17, 19, 20].

Given the advances in HIV medicine and neuroimaging techniques, we recruited virally suppressed HIV-infected individuals and a demographically comparable HIV-uninfected control

Received 3 January 2017; editorial decision 13 March 2017; accepted 29 March 2017; published online April 6, 2017.

Presented in part: Conference on Retroviruses and Opportunistic Infections, Seattle, 22–25 February 2016. Abstract 148; and British HIV Association Annual Conference, Manchester, 19–22 April 2016. Abstract 012.

^aA. W. and D. J. S. contributed equally to this work.

Correspondence: J. Underwood, Clinical Trials Centre, Winston Churchill Wing, St Mary's Hospital, London W2 1NY, UK (jonathan.underwood@imperial.ac.uk).

Clinical Infectious Diseases® 2017;65(3):422–32

© The Author 2017. Published by Oxford University Press for the Infectious Diseases Society of America. All rights reserved. For permissions, e-mail: journals.permissions@oup.com. DOI: 10.1093/cid/cix301

group into the European Union–funded Comorbidity in Relation to AIDS (COBRA) study. We determined the prevalence of cognitive impairment and its relationships with gray and white matter abnormalities. Furthermore, we systematically investigated whether previously proposed subtypes of HIV-associated brain injury [21] were present using a multimodal, “machine-learning” approach. We tested the following hypotheses: (i) despite successful ART, HIV-infected individuals would exhibit cognitive impairment compared to an appropriate HIV-uninfected control population; (ii) HIV-infected individuals would have lower gray and white matter volumes as well as multiple abnormalities on diffusion-weighted imaging; (iii) cognitive impairment would be associated with abnormal brain structure; and (iv) gray and white matter abnormalities would occur together and more commonly in HIV-infected individuals, supporting the presence of a common pathogenic mechanism.

METHODS

Participants

In total, 134 HIV-infected participants were recruited to the COBRA study from London (n = 59) and Amsterdam (n = 75). For a graphical illustration of the methods, see Supplementary Figure 1. A demographically comparable HIV-uninfected control population was recruited from sexual health clinics and specific community groups (London: n = 29; Amsterdam: n = 50). Eligible participants were aged ≥ 45 years with no significant neurological conditions, substance/alcohol abuse, or moderate/severe depression (see Supplementary Data for specific exclusion criteria). All HIV-infected participants had to have plasma HIV RNA < 50 copies/mL on ART for > 12 months prior to enrollment.

This study was approved by the institutional review board of the Academic Medical Center (NL 30802.018.09) and a UK Research Ethics Committee (13/LO/0584 Stanmore, London). All participants provided written informed consent.

Neuropsychological Tests

Participants completed a comprehensive neuropsychological test battery, assessing attention, executive function, language, memory, information processing speed, and motor function (Supplementary Table 1). Raw scores were converted to standardized T-scores accounting for age and educational level with higher T-scores representing better cognitive function. Global T-score was the mean of the 6 domain T-scores. Three common classification methods, the HIV-associated neurocognitive disorder (“Frascati”) criteria, the global deficit score (GDS), and multivariate normative comparison (MNC), were then applied according to published methods [22–24].

Neuroimaging Acquisition

In London, images were acquired using a Siemens 3T Verio scanner with a 32-channel head coil (HIV-infected: n = 59;

HIV-uninfected: n = 29) and in Amsterdam initially with a Philips 3T Intera with an 8-channel phased array head coil (HIV-infected: n = 46; HIV-uninfected: n = 20) and then using a Philips 3T Ingenia with a 16-channel head coil (HIV-infected: n = 29; HIV-uninfected: n = 30; both Philips Healthcare, Best, the Netherlands) due to a scanner upgrade (see Supplementary Data for scanning parameters).

Image Processing

T1-weighted images were pre-processed using SPM12 (University College London, United Kingdom). In brief, images were bias corrected, segmented into gray matter, white matter, and cerebrospinal fluid (CSF), and volumes calculated. These were then registered to a custom template and normalized to Montreal Neurological Institute (MNI) 152 space using the diffeomorphic anatomical registration using exponentiated lie algebra (DARTEL) algorithm [25].

Diffusion data were pre-processed using FMRIB Software Library version 5.0.6 (FSL, FMRIB, University of Oxford). In brief, images were corrected for eddy currents and head motion, nonbrain tissue was deleted, and the diffusion tensor model was fitted at every voxel. These were then registered to a custom template and standard space, using Diffusion Tensor Imaging ToolKit version 2.3.1 [26]. Fractional anisotropy (FA), and axial, mean and radial diffusivity maps for each participant were then “skeletonized” using FSL and thresholded using FA ≥ 0.2 to exclude areas with considerable interindividual variability prior to performing tract-based spatial statistics [27].

Statistical Analyses

Group Comparisons

Baseline group differences were assessed using χ^2 , Fisher exact, Wilcoxon rank-sum, and unpaired *t* tests as appropriate. To account for variance associated with potential scanner and head coil differences, a 3-level factor was entered into all models, an approach used previously in multisite studies of HIV-infected individuals [8, 20]. These analyses were performed using R software version 3.1.3, with *P* values $< .05$ considered statistically significant.

Voxelwise Inference Testing

Voxelwise group differences in gray and white matter volume and diffusion measures were calculated using the general linear model, adjusting for age, intracranial volume, and scanner. Correction for multiple comparisons used permutation testing [28] (n = 10 000) and threshold-free cluster enhancement [29]. Permutation-corrected *P* values $< .05$ were considered significant.

Combining Imaging and Cognitive Data

For each cognitive domain, a multiple linear regression model was fitted with age, intracranial volume, scanner, HIV status, and either total gray matter volume or mean

Table 1. Baseline Characteristics of the Study Cohort

Characteristic	HIV-Infected (n = 134)	HIV-Uninfected (n = 79)	P Value
Age, y, median (IQR)	55 (51–62)	57 (52–64)	.24
Gender, No. (%)			.79
Female	9 (6.7)	6 (7.6)	
Male	125 (93.3)	73 (92.4)	
Ethnicity, No. (%)			.03
Black African	16 (12.0)	2 (2.6)	
White	117 (88.0)	76 (97.4)	
Sexuality, No. (%)			.45
MSM	104 (77.6)	59 (74.7)	
Bisexual	10 (7.5)	4 (5.1)	
Heterosexual	18 (13.4)	16 (20.2)	
Years of education, median (IQR)	14 (13–16)	16 (14–17)	.23
Cardiovascular disease, No. (%)			
Hypertension ^a	56 (42.1)	30 (38.5)	.66
Myocardial infarction	2 (1.5)	3 (3.8)	.36
Type 1 diabetes	0 (0)	0 (0)	NA
Type 2 diabetes	10 (7.5)	5 (6.3)	1.00
BMI, kg/m ² , median (IQR)	24.6 (22.6–27.4)	24.6 (23.3–28.4)	.30
Total cholesterol, mmol/L, median (IQR)	5.28 (5.11–5.45)	5.33 (5.11–5.55)	.51
HDL cholesterol, mmol/L, median (IQR)	1.26 (1.07–1.50)	1.30 (1.07–1.57)	.51
LDL cholesterol, mmol/L, median (IQR)	2.99 (2.83–3.16)	3.14 (2.83–3.16)	.30
Triglycerides, mmol/L, median (IQR)	1.70 (1.15–2.53)	1.51 (1.07–2.25)	.20
Smoking status, No. (%)			.24
Current smoker	40 (29.9)	20 (25.3)	
Ex-smoker	58 (43.2)	29 (36.7)	
Never smoker	36 (26.9)	30 (38.0)	
Alcohol consumption, No. (%)			.04
Current drinker	104 (77.6)	71 (89.9)	
Previous drinker	18 (13.4)	3 (3.8)	
Never drunk	12 (9.0)	4 (5.1)	
Use of recreational drugs in past 6 mo, No. (%)	44 (32.8)	18 (22.8)	.16
CD4 ⁺ count, cells/μL, median (IQR)	618 (472–806)	900 (692–1174)	<.01
CD4 ⁺ :CD8 ⁺ cell count ratio, median (IQR)	0.84 (0.60–1.12)	2.01 (1.44–2.64)	<.01
Nadir CD4 ⁺ count, cells/μL, median (IQR)	180 (90–250)	NA	
Years since HIV diagnosis, median (IQR)	15.0 (9.1–20.0)	NA	
Duration of ART, y, median (IQR)	12.5 (7.4–16.9)	NA	
HIV RNA <200 copies/mL, No. (%)	134 (100)	NA	
Prior clinical AIDS, No. (%)	42 (31.3)	NA	
Likely route of HIV transmission, No. (%)		NA	
MSM	115 (85.8)		
Heterosexual sex	15 (11.2)		
IVDU/Blood product	1 (0.8)		
Unknown	3 (2.2)		

P values calculated using the χ^2 test, Fisher exact test, or Wilcoxon rank-sum test as appropriate.

Abbreviations: ART, antiretroviral therapy; BMI, body mass index; HDL, high-density lipoprotein; HIV, human immunodeficiency virus; IQR, interquartile range; IVDU, intravenous drug use; LDL, low-density lipoprotein; MSM, men who have sex with men, NA, not applicable.

^aHypertension was defined by either 3 measurements of systolic blood pressure ≥ 140 mm Hg, 3 measurements of diastolic blood pressure ≥ 90 mm Hg, or use of blood pressure-lowering medication.

skeleton FA as independent variables and the relevant cognitive domain T-score as the dependent variable. Separate models with an additional HIV status and imaging measure interaction term were also tested. To investigate the relationship between localized brain structure and cognitive function, voxelwise regressions were calculated using similar methods.

Cluster Analysis

T1 weighting provides good contrast between gray and white matter for volumetric assessment, whereas diffusion weighting provides information about white matter microstructure. To take advantage of this complementary information, we used multivariate k-means clustering to test whether distinct groups could be identified based on

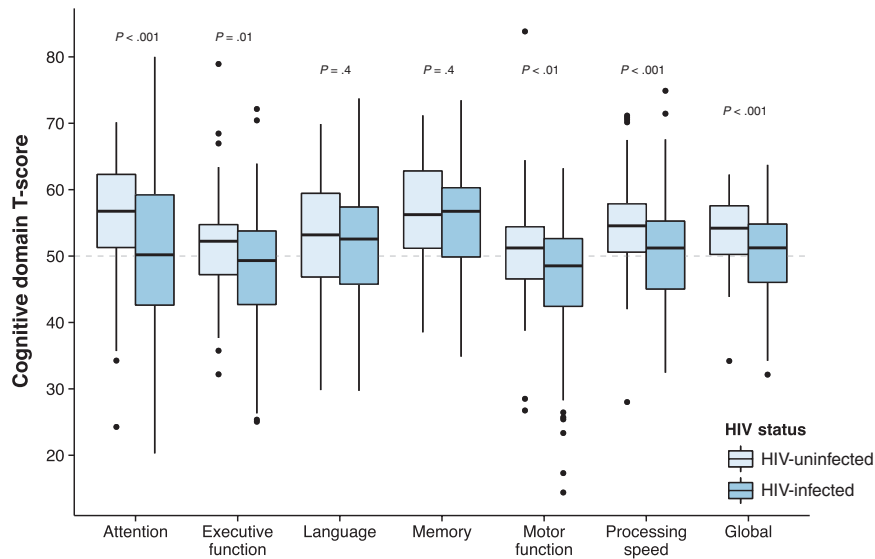


Figure 1. Boxplots of demographically adjusted cognitive domain T-scores by human immunodeficiency virus (HIV) status. P-values calculated using the Wilcoxon rank-sum test.

neuroimaging measures. As a dimension reduction step, each participant's brain was summarized into 109 regions using the Harvard-Oxford and International Consortium of Brain Mapping DTI-81 atlases. To ensure comparable distributions, these were then scaled before entering into the clustering model. To assess the optimal number of clusters, separate models with 2–10 clusters were calculated. These were compared using the Calinski-Harabasz index and the average silhouette width. The Duda-Hart test was used to confirm cluster structure to the data (ie, $k > 1$). Cluster stability was assessed using the Jaccard coefficient, calculated using bootstrapping with 10 000 resamples [30]. Cluster analyses were performed with the R package “fpc” version 2.1.9.

RESULTS

Participants

At entry, all HIV-infected participants ($n = 134$) had an undetectable plasma HIV RNA with a median $CD4^+$ cell count of 618 (interquartile range [IQR], 472–806) cells/ μ L and duration of ART of 12.5 (IQR, 7.4–16.9) years. The HIV-uninfected group ($n = 79$) was comparable to the HIV-infected group in age, sex, education level, cardiovascular risk factors, smoking, and recreational drug use. The HIV-infected group included a greater proportion of black Africans (Table 1). One participant did not complete the full cognitive battery, and neuroimaging data were missing for 5 participants (T1 not useable, $n = 1$; incomplete diffusion MRI, $n = 1$; excessive motion artefact on diffusion MRI, $n = 3$).

Table 2. Volumetric and Diffusion Imaging Measurements

Imaging Measure	Volumetric Measures			t_{206}	PValue
	HIV-Infected	HIV-Uninfected	Difference (95% CI)		
Gray matter volume, mL	659	673	13.7 (2.3–25.1)	2.37	.02
White matter volume, mL	479	476	2.4 (–6.4 to 11.2)	–0.54	.59
Imaging Measure	Diffusion Measures			t_{202}	PValue
	HIV-Infected	HIV-Uninfected	Difference (95% CI)		
Fractional anisotropy	0.477	0.484	0.007 (.002–.012)	2.92	<.01
Mean diffusivity, mm^2/s	705	696	8.5 (1.2–15.8)	–2.27	.02
Radial diffusivity, mm^2/s	503	493	10.3 (2.7–17.9)	–2.66	<.01
Axial diffusivity, mm^2/s	1108	1103	4.9 (–2.5 to 12.3)	–1.31	.19

Least squares means, a potentially better estimate of the true population mean for each neuroimaging measure by HIV status and 95% CIs, adjusted for age, intracranial volume, and scanner type. Subscript indicates degrees of freedom for the t-statistic.

Abbreviations: CI, confidence interval; HIV, human immunodeficiency virus.

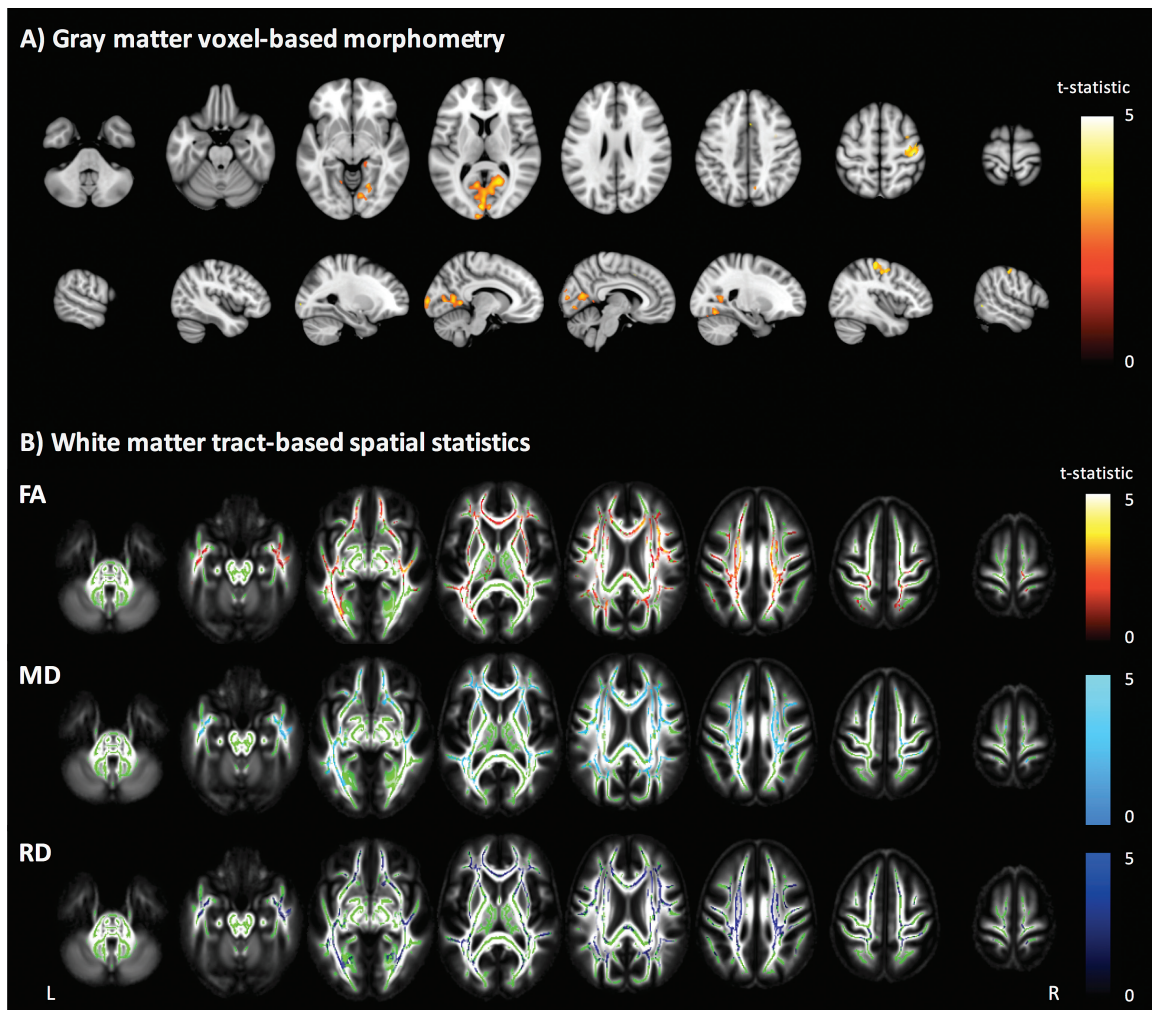


Figure 2. Voxelwise analyses of volumetric and diffusion measures. *A*, Gray matter voxel-based morphometry group comparison. Areas with significantly ($P < .05$) lower gray matter volume colored by t-statistic (red/yellow), corrected for multiple comparisons and adjusted for age, intracranial volume, and scanner. Significant differences are overlaid on the Montreal Neurological Institute 152 T1 brain image. *B*, White matter tract-based spatial statistics group comparison. Areas of significantly ($P < .05$) lower fractional anisotropy (FA), higher mean diffusivity (MD), and higher radial diffusivity (RD) are colored red-yellow, light blue, and dark blue, respectively, by t-statistic, corrected for multiple comparisons, and adjusted for age, intracranial volume, and scanner. Significant differences overlaid on the white matter skeleton (green) and the mean fractional anisotropy image (grayscale).

Cognitive Function

Cognitive impairment was more prevalent in the HIV-infected group, regardless of the method used: GDS: 18.0% vs 3.8% (odds ratio [OR], 5.58; 95% confidence interval [CI], 1.86–24.1; $P < .01$); Frascati: 18.0% vs 3.8% (OR, 5.58; 95% CI, 1.86–24.1; $P < .01$); MNC: 19.5% vs 2.5% (OR, 9.36; 95% CI, 2.68–59.2; $P < .001$). The HIV-infected group scored lower than the control group in the domains of attention, executive function, motor function, and processing speed (Figure 1; $W_{210} > 6300$ and $P \leq .01$ for all). Only 1.5% of the HIV-infected group and 1.2% of controls fulfilled the criteria for HIV-associated dementia.

Brain Tissue Volumes and Diffusion Measures

HIV-infected individuals had lower total gray matter volume than controls (Table 2). There was a significant negative

correlation between age and gray matter volume ($r = -0.31$; $P < .0001$) but no significant age and HIV status interaction ($t_{205} = 0.45$; $P = .65$). Voxelwise analysis demonstrated lower gray matter volume in the HIV-infected group, located principally in the intracalcarine and supracalcarine cortices (Figure 2). In contrast, total white matter volume was not significantly different between the groups ($P = .59$), nor were there any significant voxelwise differences.

Despite comparable white matter volumes, HIV-infected individuals had lower FA and higher mean and radial (but not axial) diffusivity than controls (Table 2). There were age-associated changes to all diffusion metrics ($r = -0.36, 0.45, 0.45$, and 0.40 for FA and mean, radial, and axial diffusivity, respectively; $P < .0001$ for all) but no significant interactions between age and HIV status ($P > .5$ for all). Voxelwise analyses revealed

Table 3. Associations Between Cognitive Function and Imaging Parameters

Cognitive Domain	Gray Matter Volume Regression Estimate (T-score/mL)			HIV-Gray Matter Interaction	
	Estimate	(95% CI)	PValue	t ₂₀₃	PValue
Attention	0.035	(-.001 to .072)	.06	1.91	.06
Executive function	0.041	(.013-.068)	<.01	0.75	.45
Memory	0.010	(-.016 to .037)	.43	-0.67	.50
Motor function	0.029	(.001-.057)	.04	0.69	.49
Processing speed	0.017	(-.010 to .043)	.21	0.76	.45
Global	0.026	(.006-.046)	.01	1.34	.18

	Fractional Anisotropy Regression Estimate (T-score/Unit FA)			HIV-Fractional Anisotropy Interaction	
	Estimate	(95% CI)	PValue	t ₁₉₉	PValue
Attention	0.099	(.013-.187)	.03	-1.67	.09
Executive function	0.073	(.008-.139)	.03	-0.62	.54
Memory	0.035	(-.028 to .097)	.27	-0.53	.60
Motor function	0.079	(.013-.144)	.02	1.25	.21
Processing speed	0.092	(.031-.152)	<.01	-0.41	.68
Global	0.062	(.014-.110)	.01	-0.63	.53

Multiple linear regression estimates for gray matter volume and FA by cognitive domain adjusted for age, intracranial volume, and scanner type. In addition, HIV status and neuroimaging measure interaction statistics for each cognitive domain are shown.

Abbreviations: CI, confidence interval; FA, fractional anisotropy; HIV, human immunodeficiency virus.

widespread abnormalities in FA, mean diffusivity, and radial diffusivity in HIV-infected individuals with a similar pattern of change to the whole brain diffusion metrics (Figure 2).

In the HIV-infected group, gray and white matter volumes and mean FA were not associated with known duration of untreated HIV infection, duration of ART, current or nadir CD4⁺ cell counts, or CD4⁺:CD8⁺ cell count ratio ($P > .15$ for all). However, there were trends for patients with prior AIDS to have lower gray matter volume (difference, 14.3 mL; $t_{128} = 1.9$; $P = .06$) and lower mean FA (difference, 0.0059; $t_{128} = 1.7$; $P = .08$).

HIV-Associated Brain Injury and Cognitive Function

Across patients and controls, larger gray matter volumes were associated with better cognitive performance. Total gray matter volume was positively correlated with executive function, motor function, and global T-scores with no significant interactions between HIV status and cognitive T-scores (Table 3). Voxelwise analyses were then performed allowing regional differences in the relationship between brain structure and cognition to be explored. Spatial correspondence between the regions of gray matter correlated with cognitive function and the previously described HIV-associated gray matter volume reduction was generally modest, but greatest for executive function (Figure 3 and Supplementary Table 2).

Across both groups, higher FA was associated with greater cognitive performance. FA averaged across the main white matter tracts was positively correlated with attention, executive function, processing speed, and global T-scores

(Table 3). There were no interactions between HIV status, FA, and cognitive T-scores. Across both groups, using a voxelwise approach, FA was positively correlated with attention, executive function, motor function and processing speed, and global T-scores in many regions, primarily in the body and genu of the corpus callosum. In contrast to the gray matter volume results, these were similar to white matter tracts with reduced FA in the HIV-infected group (Figure 3 and Supplementary Table 2).

Cluster Analysis

Using k-means clustering, 2 groups were identified that were stable with resampling (mean Jaccard coefficient = 0.99). Other cluster models (ie, $k > 2$) were much less stable (mean Jaccard coefficient < 0.7). In the 2-cluster model, cluster 1 ($n = 99$) had higher gray matter volume and higher mean FA in all regions, whereas cluster 2 ($n = 109$) had lower gray matter volume and lower mean FA in all regions. HIV-infected individuals were more likely to be members of cluster 2 (61.2% vs 36.4%; OR, 2.74; 95% CI, 1.53–4.98; $P < .001$, Figure 4). Furthermore, subjects in cluster 2 were older (median, 59.3 vs 54.6 years; $W_{206} = 3634$; $P < .001$) and had significantly poorer cognitive function in the domains of attention, executive function, motor function, and processing speed (Figure 5; $W_{205} \geq 6307$; $P \leq .03$ for all). Importantly, these cognitive differences between members of clusters 1 and 2 were not due to demographic differences, as the cognitive T-scores are adjusted for age and educational level. Although there were no significant differences in current and nadir CD4⁺

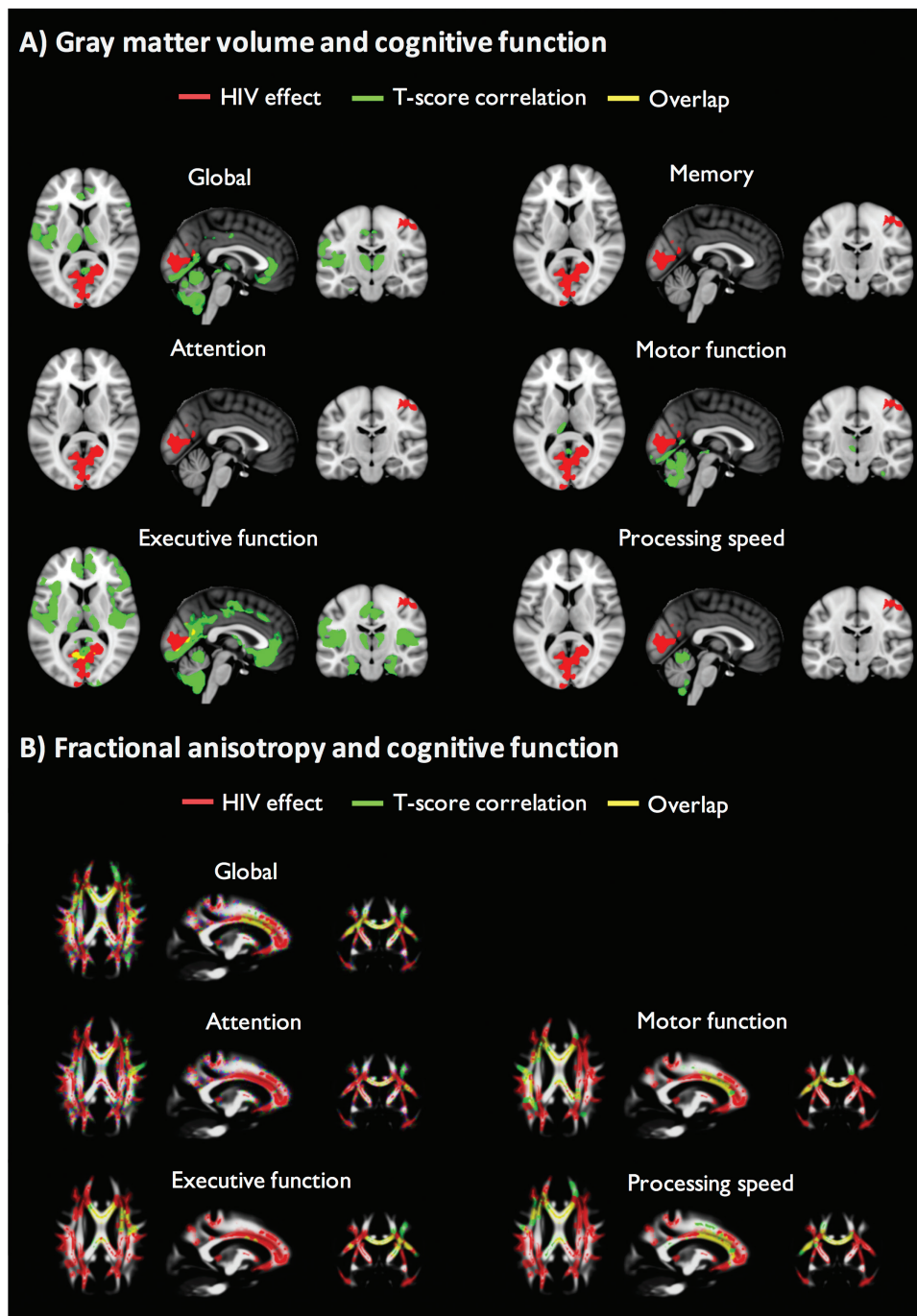


Figure 3. Correspondence between human immunodeficiency virus (HIV)-associated brain injury and regions correlated with cognitive function. *A*, Voxel-wise analysis depicting regions of gray matter volume significantly lower in the HIV-infected group vs HIV-uninfected group (red), positively correlated with cognitive function T-scores (green) and overlap (yellow), corrected for multiple comparisons and adjusted for age, intracranial volume, and scanner. Statistical images overlaid on MNI 152 T1. There were no voxelwise associations between language T-scores and gray matter volume. *B*, Voxel-wise analyses depicting regions of fractional anisotropy (FA) significantly lower in the HIV-infected group vs HIV-uninfected group (red), positively correlated with cognitive function T-scores (green) and overlap (yellow), corrected for multiple comparisons and adjusted for age, intracranial volume, and scanner. Statistical images overlaid on the mean FA image. There were no voxelwise associations between language or memory T-scores and FA.

cell counts ($P = .10$ and $.17$, respectively), HIV-infected individuals in cluster 2 had lower CD4⁺:CD8⁺ ratios (0.82 vs 1.06; $W_{132} = 2666$; $P = .01$) and were older (58.6 vs 53.2 years; $W_{132} = 1380$; $P < .001$) than those in cluster 1.

DISCUSSION

We demonstrate that HIV-infected individuals have evidence of cognitive impairment, lower gray matter volume, and widespread white matter microstructural abnormalities despite

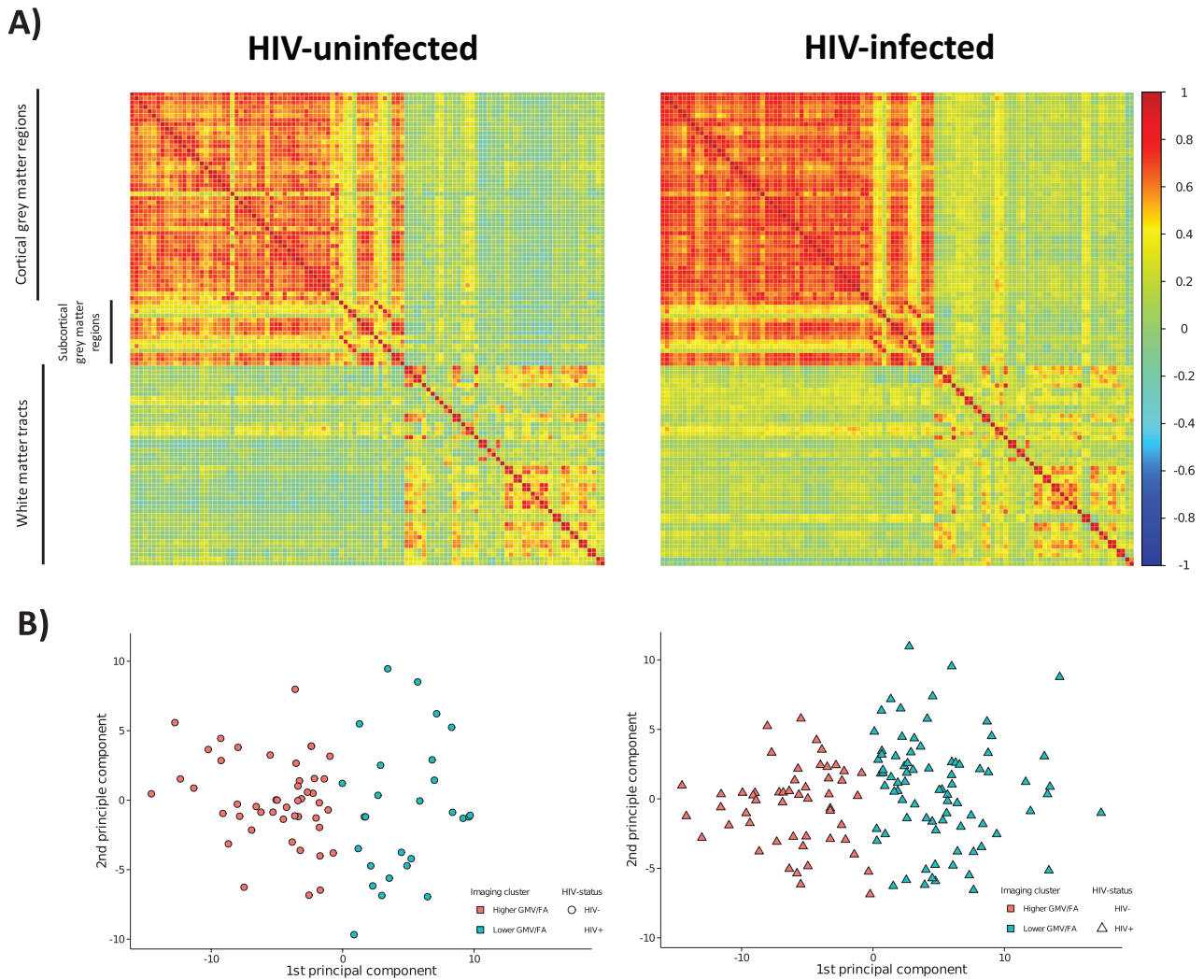


Figure 4. K-means cluster analysis results by human immunodeficiency virus (HIV) status. *A*, Visualization of the correlation matrices for the regions of cortical and subcortical gray matter volume (GMV; Harvard-Oxford atlas) and white matter fractional anisotropy (FA) (International Consortium of Brain Mapping DTI-81 white matter labels) used in the k-means clustering analysis for the HIV-infected and HIV-uninfected groups. The correlation coefficient is represented by the color of the box (scale to the right of the figure). *B*, Principal component plots showing the separation of the clusters based on the k-means clustering analysis of parcellated gray matter and mean FA data for the HIV-uninfected controls on the left (circles) and HIV-infected participants on the right (triangles). Cluster 1 (orange) had higher GMV and higher FA for each region whereas cluster 2 (green) had lower GMV and lower FA for each region. HIV-infected individuals were more likely to be members of the lower GMV and lower FA cluster (odds ratio, 2.74; 95% confidence interval, 1.53–4.98).

successful ART. Generally, the gray matter volume reduction associated with HIV infection was modest and did not occur in regions where brain structure correlated with cognitive function. In contrast, HIV-associated white matter abnormalities were widespread and found in many of the white matter tracts whose structure correlated with cognitive function. These findings extend previous work [13, 17, 19, 20] by showing that white matter structure is correlated with cognitive impairment in chronic HIV infection. Our findings suggest that the pathophysiology of cognitive impairment in treated HIV disease is predominantly due to white matter microstructural injury and support the use of FA as a biomarker to identify HIV-associated brain injury. Furthermore, we consistently showed a lack of

interaction between HIV status, age, and neuroimaging biomarkers, which suggests static rather than active brain injury in well-treated patients. However, longitudinal data are required to confirm this.

The prevalence of cognitive impairment in well-treated HIV-infected patients has been uncertain. Although early studies reported high rates of cognitive impairment in chronically treated patients [5, 6, 31], some studies have failed to observe this [32]. In our study, both study groups were high performing, with nearly 40% having some form of tertiary education, which may explain the relatively low prevalence of cognitive impairment. Furthermore, the use of methods less likely to classify high numbers of individuals with cognitive impairment such

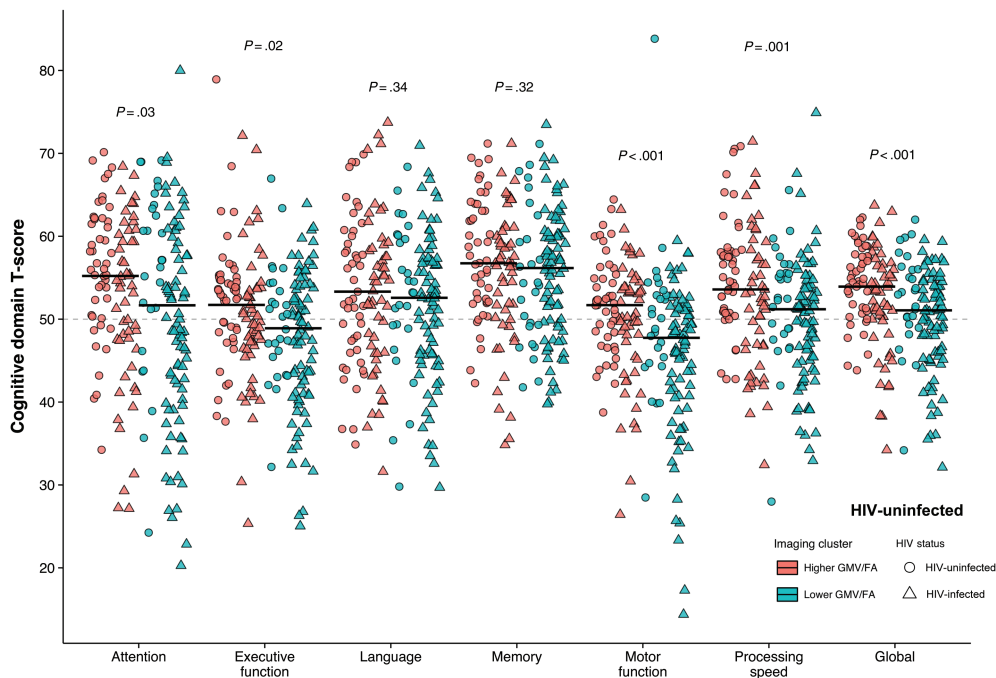


Figure 5. K-means cluster analysis and cognitive function by human immunodeficiency virus (HIV) status. Jitterplot of cognitive domain T-scores grouped by k-means cluster analysis. Cluster 1 represents the cluster with higher total gray matter volume (GMV) and higher mean white matter skeleton fractional anisotropy (FA) in each region, whereas cluster 2 represents the cluster with lower total GMV and lower mean white matter skeleton FA in each region. Black lines represent medians for each cluster with *P* values calculated using the Wilcoxon rank-sum test.

as MNC [33], in comparison with a demographically comparable control group and sustained suppression of viremia in the patient group, is likely to have contributed to the relatively low prevalence of HIV-associated cognitive impairment.

Total gray matter volume was lower in the HIV-infected group with reductions occurring primarily in the intracalcarine and supracalcarine cortices. Previous studies in populations with variable suppression of HIV replication have described more widespread gray matter volume reductions [8, 10, 12]. However, the locations where we observed abnormalities are consistent with regions of greatest neuronal [34] and gray matter volume [11] loss observed in untreated HIV infection. Together with the trend for those with prior AIDS to have the lowest gray matter volume, our findings suggest these regions are the earliest affected during the course of HIV infection and that further atrophy may be prevented with successful treatment.

Diffusion-weighted imaging showed widespread evidence of HIV-associated white matter microstructural injury, with the disparity in radial but not axial diffusivity suggestive of white matter demyelination [35]. The characteristics and location of this injury are consistent with histopathological reports from the pre-ART era, where myelin damage was found in the central white matter [36]. The decoupling of diffusion abnormalities and white matter atrophy is interesting and has been reported previously in HIV-infected individuals with relatively preserved immunity (mean CD4⁺ count, 613

cells/uL) [17]. Together with the trend for the most severe abnormalities to occur in patients with prior AIDS, our findings suggest that diffusion abnormalities may reflect historical damage prior to ART initiation and that progression to white matter atrophy may be aborted with sustained suppression of HIV replication. Although cardiovascular disease may also be implicated in well-treated patients [37], this is unlikely to explain the observed group differences, given the similarity in measured cardiovascular risk factors between groups. As we report cross-sectional data, we are unable to resolve the issue of whether these imaging changes reflect historical damage or an ongoing pathological process.

The HIV-associated microstructural injury occurred in white matter tracts correlated with cognitive function. In contrast, the HIV-associated gray matter volume reduction generally did not occur in brain regions correlated with cognitive function. Although this could reflect the cognitive battery we employed, these data suggest that white matter abnormalities may be a more important determinant of cognitive impairment in treated HIV disease. White matter abnormalities of this type correlate with cognitive function in other disease states [38], and are thought to disrupt the synchronized functioning of large-scale, distributed brain networks that cognition depends on.

Using a multivariate approach to examine individual differences in volumetric and diffusion data simultaneously, we identified a brain phenotype that was associated with aging,

cognitive dysfunction, and HIV status. Furthermore, this phenotype was associated with lower CD4⁺:CD8⁺ ratios. This biomarker of immune activation has previously been associated with other age-related comorbidities in well-treated cohorts [39]. Our findings suggest that persistent immune activation may also be associated with brain injury, which may reflect the legacy of prolonged untreated infection as normalization of this ratio has been associated with earlier ART initiation [40].

Our study benefits from comprehensive neuropsychological, volumetric, and diffusion assessments in patients and demographically appropriate controls. However, our study has a number of limitations. Although our cohort is not representative of the entire HIV-infected population, it is representative of older HIV-infected adults receiving care in a Northern European setting where >90% are successfully treated [7]. Cohort studies are potentially limited by unmeasured differences confounding group comparisons. This is particularly an issue when studying HIV-infected populations and age-related comorbidities given high rates of smoking, alcohol, and recreational drug use. We limited this by recruiting a comparable control population, but unmeasured differences between the 2 groups may remain. One previous study of virally suppressed patients [41], which used different MRI modalities, may have had a less comparable control group (81% of the HIV-infected group vs 47% of the HIV-uninfected group was male), which may lead to an overstatement of the HIV association. Differences in scanner and head coil parameters between sites may potentially confound multisite neuroimaging studies; however, bias was minimized by adjusting for these factors in our models. Furthermore, restricting the analyses to data acquired in London only resulted in HIV associations of a similar magnitude and direction as the entire study population (Supplementary Table 3), giving confidence that scanner differences did not bias our main findings. Cluster analysis may split the participants into potentially arbitrary groups and the “good”/“bad” brain phenotype may, in reality, be more of a continuum. Although exploratory, we found excellent internal validity by demonstrating a high level of cluster stability with resampling and good external validity by the associations of cluster membership with age, HIV status, cognitive function, and markers of systemic immune activation.

To conclude, HIV infection was associated with both lower gray matter volume and white matter microstructural injury. Cognitive impairment, present in approximately 20% of cases, was most clearly associated with white matter abnormalities. Gray and white matter abnormalities tended to occur together, suggesting a common etiology for HIV-associated brain injury, which may be related to prolonged untreated infection and immune activation, in common with other non-AIDS comorbidities.

Supplementary Data

Supplementary materials are available at *Clinical Infectious Diseases* online. Consisting of data provided by the authors to benefit the reader, the posted materials are not copyedited and are the sole responsibility of the authors, so questions or comments should be addressed to the corresponding author.

Notes

Acknowledgments. We thank all the participants in the study for their time and effort. We also thank the Pharmacokinetic and Clinical Observations in People Over Fifty (POPPY) study and the Comorbidity and Aging With HIV (AGEHIV) study teams at their respective sites (see Appendix).

Financial support. This work was supported by a European Union Seventh Framework Programme grant to the COBRA project (FP-7-HEALTH 305522, all authors); National Institute for Health Research (NIHR) Professorship (NIHR-RP-011-048; D. J. S.), NIHR Imperial Biomedical Research Centre; the Netherlands Organisation for Health Research and Development (ZonMW) (grant number 300020007); Stichting AIDS Fonds (grant number 2009063); Nuts-Ohra Foundation (grant number 1003-026); and unrestricted scientific grants from ViiV Healthcare, Gilead Sciences, Janssen Pharmaceutica N.V., Bristol-Myers Squibb (BMS), and Merck & Co to the AGE_hIV cohort study, as well as investigator-initiated grants from BMS, Gilead Sciences, Janssen, Merck, and ViiV Healthcare to the POPPY cohort study.

Potential conflicts of interest. A. W. has received honoraria or research grants from or been a consultant or investigator in clinical trials sponsored by Abbott, Boehringer Ingelheim, BMS, Gilead Sciences, GlaxoSmithKline, Janssen-Cilag, Roche, Pfizer, and ViiV Healthcare. P. R. reports grants from Gilead Sciences, ViiV Healthcare, Janssen Pharmaceutica, BMS, and Merck & Co; and other from Gilead Sciences, Janssen Pharmaceutica, and ViiV Healthcare. R. A. Z. has received travel grants from BMS and Gilead Sciences, and was a speaker at an event sponsored by Gilead Sciences for which her institution received remuneration. All other authors report no potential conflicts. All authors have submitted the ICMJE Form for Disclosure of Potential Conflicts of Interest. Conflicts that the editors consider relevant to the content of the manuscript have been disclosed.

References

1. May MT, Gompels M, Delpech V, et al; UK Collaborative HIV Cohort (UK CHIC) Study. Impact on life expectancy of HIV-1 positive individuals of CD4⁺ cell count and viral load response to antiretroviral therapy. *AIDS* **2014**; *28*:1193–202.
2. Schouten J, Wit FW, Stolte IG, et al; AGEHIV Cohort Study Group. Cross-sectional comparison of the prevalence of age-associated comorbidities and their risk factors between HIV-infected and uninfected individuals: the AGEHIV cohort study. *Clin Infect Dis* **2014**; *59*:1787–97.
3. Lescure FX, Omland LH, Engsig FN, et al. Incidence and impact on mortality of severe neurocognitive disorders in persons with and without HIV infection: a Danish nationwide cohort study. *Clin Infect Dis* **2011**; *52*:235–43.
4. Hinkin CH, Castellon SA, Durvasula RS, et al. Medication adherence among HIV+ adults: effects of cognitive dysfunction and regimen complexity. *Neurology* **2002**; *59*:1944–50.
5. Heaton RK, Franklin DR, Ellis RJ, et al; CHARTER Group; HNRC Group. HIV-associated neurocognitive disorders before and during the era of combination antiretroviral therapy: differences in rates, nature, and predictors. *J Neurovirol* **2011**; *17*:3–16.
6. Robertson KR, Smurzynski M, Parsons TD, et al. The prevalence and incidence of neurocognitive impairment in the HAART era. *AIDS* **2007**; *21*:1915–21.
7. Public Health England. HIV in the United Kingdom: 2014 report. UK: Public Health England, **2014**. Available at https://www.gov.uk/government/uploads/system/uploads/attachment_data/file/401662/2014_PHE_HIV_annual_report_draft_Final_07-01-2015.pdf.
8. Becker JT, Maruca V, Kingsley LA, et al. Factors affecting brain structure in men with HIV disease in the post-HAART era. *Neuroradiology* **2012**; *54*:113–21.
9. Towgood KJ, Pitkanen M, Kulasegaram R, et al. Mapping the brain in younger and older asymptomatic HIV-1 men: frontal volume changes in the absence of other cortical or diffusion tensor abnormalities. *Cortex* **2012**; *48*:230–41.

10. Chiang MC, Dutton RA, Hayashi KM, et al. 3D pattern of brain atrophy in HIV/AIDS visualized using tensor-based morphometry. *Neuroimage* **2007**; 34:44–60.
11. Thompson PM, Dutton RA, Hayashi KM, et al. Thinning of the cerebral cortex visualized in HIV/AIDS reflects CD4+ T lymphocyte decline. *Proc Natl Acad Sci U S A* **2005**; 102:15647–52.
12. Küper M, Rabé K, Esser S, et al. Structural gray and white matter changes in patients with HIV. *J Neurol* **2011**; 258:1066–75.
- 13.ANCES BM, Ortega M, Vaida F, Heaps J, Paul R. Independent effects of HIV, aging, and HAART on brain volumetric measures. *J Acquir Immune Defic Syndr* **2012**; 59:469–77.
14. Corrêa DG, Zimmermann N, Doring TM, et al. Diffusion tensor MR imaging of white matter integrity in HIV-positive patients with planning deficit. *Neuroradiology* **2015**; 57:475–82.
15. Leite SC, Corrêa DG, Doring TM, et al. Diffusion tensor MRI evaluation of the corona radiata, cingulate gyri, and corpus callosum in HIV patients. *J Magn Reson Imaging* **2013**; 38:1488–93.
16. Nir TM, Jahanshad N, Busovaca E, et al. Mapping white matter integrity in elderly people with HIV. *Hum Brain Mapp* **2014**; 35:975–92.
17. Stebbins GT, Smith CA, Bartt RE, et al. HIV-associated alterations in normal-appearing white matter. *J Acquir Immune Defic Syndr* **2007**; 46:564–73.
18. Stubbe-Drger B, Deppe M, Mohammadi S, et al. Early microstructural white matter changes in patients with HIV: a diffusion tensor imaging study. *BMC Neurol* **2012**; 12:23.
19. Su T, Caan MWA, Wit FWNM, et al; AGEHIV Cohort Study. White matter structure alterations in HIV-1-infected men with sustained suppression of viraemia on treatment. *AIDS* **2015**; 30:311–22.
20. Jernigan TL, Archibald SL, Fennema-Notestine C, et al; CHARTER Group. Clinical factors related to brain structure in HIV: the CHARTER study. *J Neurovirol* **2011**; 17:248–57.
21. Brew BJ. Evidence for a change in AIDS dementia complex in the era of highly active antiretroviral therapy and the possibility of new forms of AIDS dementia complex. *AIDS* **2004**; 18:75.
22. Antinori A, Arendt G, Becker JT, et al. Updated research nosology for HIV-associated neurocognitive disorders. *Neurology* **2007**; 69:1789–99.
23. Carey CL, Woods SP, Gonzalez R, et al; HNRC Group. Predictive validity of global deficit scores in detecting neuropsychological impairment in HIV infection. *J Clin Exp Neuropsychol* **2004**; 26:307–19.
24. Huizenga HM, Smeding H, Grasman RP, Schmand B. Multivariate normative comparisons. *Neuropsychologia* **2007**; 45:2534–42.
25. Ashburner J. A fast diffeomorphic image registration algorithm. *NeuroImage* **2007**; 38:95–113.
26. Wang Y, Gupta A, Liu Z, et al. DTI registration in atlas based fiber analysis of infantile Krabbe disease. *Neuroimage* **2011**; 55:1577–86.
27. Smith SM, Jenkinson M, Johansen-Berg H, et al. Tract-based spatial statistics: voxelwise analysis of multi-subject diffusion data. *Neuroimage* **2006**; 31:1487–505.
28. Winkler AM, Ridgway GR, Webster MA, Smith SM, Nichols TE. Permutation inference for the general linear model. *Neuroimage* **2014**; 92:381–97.
29. Smith SM, Nichols TE. Threshold-free cluster enhancement: addressing problems of smoothing, threshold dependence and localisation in cluster inference. *Neuroimage* **2009**; 44:83–98.
30. Hennig C. Cluster-wise assessment of cluster stability. *Comput Stat Data An* **2007**; 52:258–71.
31. Heaton RK, Clifford DB, Franklin DR Jr, et al; CHARTER Group. HIV-associated neurocognitive disorders persist in the era of potent antiretroviral therapy: CHARTER Study. *Neurology* **2010**; 75:2087–96.
32. McDonnell J, Haddow L, Daskalopoulou M, et al; Cognitive Impairment in People With HIV in the European Region (CIPHER) Study Group. Minimal cognitive impairment in UK HIV-positive men who have sex with men: effect of case definitions and comparison with the general population and HIV-negative men. *J Acquir Immune Defic Syndr* **2014**; 67:120–7.
33. Su T, Schouten J, Geurtsen GJ, et al; AGEHIV Cohort Study Group. Multivariate normative comparison, a novel method for more reliably detecting cognitive impairment in HIV infection. *AIDS* **2015**; 29:547–57.
34. Everall IP, Luthert PJ, Lantos PL. Neuronal number and volume alterations in the neocortex of HIV infected individuals. *J Neurol Neurosurg Psychiatry* **1993**; 56:481–6.
35. Song SK, Sun SW, Ju WK, Lin SJ, Cross AH, Neufeld AH. Diffusion tensor imaging detects and differentiates axon and myelin degeneration in mouse optic nerve after retinal ischemia. *Neuroimage* **2003**; 20:1714–22.
36. Gray F, Lesca MC, Keohane C, et al. Early brain changes in HIV infection: neuropathological study of 11 HIV seropositive, non-AIDS cases. *J Neuropathol Exp Neurol* **1992**; 51:177–85.
37. Brew BJ. Has HIV-associated neurocognitive disorders now transformed into vascular cognitive impairment? *AIDS* **2016**; 30:2379–80.
38. Medina D, DeToledo-Morrell L, Urresta F, et al. White matter changes in mild cognitive impairment and AD: a diffusion tensor imaging study. *Neurobiol Aging* **2006**; 27:663–72.
39. Mussini C, Lorenzini P, Cozzi-Lepri A, et al; Icona Foundation Study Group. CD4/CD8 ratio normalisation and non-AIDS-related events in individuals with HIV who achieve viral load suppression with antiretroviral therapy: an observational cohort study. *Lancet HIV* **2015**; 2:e98–106.
40. Serrano-Villar S, Sainz T, Lee SA, et al. HIV-infected individuals with low CD4/CD8 ratio despite effective antiretroviral therapy exhibit altered T cell subsets, heightened CD8+ T cell activation, and increased risk of non-AIDS morbidity and mortality. *PLoS Pathog* **2014**; 10:e1004078.
41. Granziera C, Daducci A, Simioni S, et al. Micro-structural brain alterations in aviremic HIV+ patients with minor neurocognitive disorders: a multi-contrast study at high field. *PLoS One* **2013**; 8:e72547.

APPENDIX

We thank the POPPY and AGE_hIV study teams at their respective sites:

Academisch Medisch Centrum, Universiteit van Amsterdam—Department of Global Health and Amsterdam Institute for Global Health and Development: P. Reiss, F. W. N. M. Wit, J. Schouten, K. W. Kooij, R. A. van Zoest, B. C. Elsenga, F. R. Janssen, M. Heidenrijk, W. Zikkenheiner. Division of Infectious Diseases: M. van der Valk. Department of Experimental Immunology: N. A. Kootstra, A. M. Harskamp-Holwerda, I. Maurer, M. M. Mangas Ruiz, A. F. Girigorie. Department of Medical Microbiology: J. Villaudy, E. Frankin, A. Pasternak, B. Berkhout, T. van der Kuyl. Department of Neurology: P. Portegies, B. A. Schmand, G. J. Geurtsen, J. A. ter Stege, M. Klein Twennaar. Department of Radiology: C.B.L.M. Majoie, M.W.A. Caan, T. Su. Department of Cell Biology: K. Weijer. Division of Endocrinology and Metabolism: P. H. L. T. Bisschop. Department of Experimental Neuroendocrinology: A. Kalsbeek. Department of Ophthalmology: M. Wezel. Department of Psychiatry: I. Visser, H. G. Ruhé. *Alma Mater Studiorum Universita di Bologna*—Department of Experimental, Diagnostic and Specialty Medicine: C. Franceschi, P. Garagnani, C. Pirazzini, M. Capri, F. Dall’Olio, M. Chiricolo, S. Salvioli. *Erasmus Universitair Medisch Centrum Rotterdam*—Department of Genetics: J. Hoeijmakers, J. Pothof. *GGD Amsterdam/Public Health Service Amsterdam*—Cluster of Infectious Diseases, research department: M. Prins, M. Martens, S. Moll, J. Berkel, M. Totté, S. Kovalev. *Göteborgs Universitet*—M. Gisslén, D. Fuchs, H. Zetterberg. *Imperial College of Science, Technology and Medicine*—Department of Medicine, Division of Infectious Diseases: A. Winston, J. Underwood, L. McDonald, M. Stott, K. Legg, A. Lovell, O. Erlwein, N. Doyle, C. Kingsley. Department of Medicine, Division of Brain Sciences, The Computational, Cognitive & Clinical Neuroimaging Laboratory: D. J. Sharp, R. Leech, J. H. Cole.

Stichting HIV Monitoring—S. Zaheri, M. M. J. Hillebregt, Y. M. C. Ruijs, D. P. Benschop. *Stichting Katholieke Universiteit Nijmegen*—D. Burger, M. de Graaff-Teulen.

Università degli studi di Modena e Reggio Emilia—Department of Medical and Surgical Sciences for Children & Adults: G. Guaraldi. *Universität Konstanz*—Department of Biology: A. Bürkle, T. Sindlinger, M. Moreno-Villanueva, A. Keller. *University College London*—Research Department of Infection and Population Health: C. Sabin, D. de Francesco. *Vlaams Instituut voor Biotechnologie*—Inflammation research center: C. Libert, S. Dewaele.